Published in final edited form as:
J Clin Immunol. 2011 December ; 31(6): 985–997. doi:10.1007/s10875-011-9574-y.

Cardiac Autoantibodies from Patients Affected by a New Variant of Endemic Pemphigus Foliaceus in Colombia, South America

Ana Maria Abreu-Velez,
Georgia Dermatopathology Associates, Atlanta, Georgia, USA

Michael S. Howard,
Georgia Dermatopathology Associates, Atlanta, Georgia, USA

Zhe Jiao,
Department of Cardiology, Emory University Medical Center, Atlanta, Georgia, USA

Weiqing Gao,
Department of Ophthalmology, Emory University Medical Center, Atlanta, Georgia, USA

Hong Yi,
Robert P. Apkarian Integrated Electron Microscopy Core, Emory University Medical Center, Atlanta, Georgia, USA

Hans E. Grossniklaus,
Department of Ophthalmology, Emory University Medical Center, Atlanta, Georgia, USA

Mauricio Duque-Ramírez, and
Chief Cardiac Electrophysiology Las Americas Clinic, Chief Cardiology General Hospital of Medellin, and Chief Section of Cardiology, CES, Medellin, Colombia

Samuel C. Dudley Jr.
Chief Section of Cardiology, University of Illinois at Chicago (UIC) Medical Center, Chicago, USA

Ana Maria Abreu-Velez: abreuvelez@yahoo.com

Abstract

Several patients affected by a new variant of endemic pemphigus foliaceus in El Bagre, Colombia (El Bagre-EPF) have experienced a sudden death syndrome, including persons below the age of 50. El Bagre-EPF patients share several autoantigens with paraneoplastic pemphigus patients, such as reactivity to plakins. Further, paraneoplastic pemphigus patients have autoantibodies to the heart. Therefore, we tested 15 El Bagre-EPF patients and 15 controls from the endemic area for autoreactivity to heart tissue using direct and indirect immunofluorescence, confocal microscopy, immunohistochemistry, immunoblotting, and immunoelectron microscopy utilizing heart extracts as antigens. We found that 7 of 15 El Bagre patients exhibited a polyclonal immune response to several cell junctions of the heart, often colocalizing with known markers. These colocalizing markers included those for the area composita of the heart, such as anti-desmoplakins I and II; markers for gap junctions, such as connexin 43; markers for tight junctions, such as ezrin and junctional adhesion molecule A; and adherens junctions, such pan-cadherin. We also detected colocalization of the patient antibodies within blood vessels, Purkinje fibers, and cardiac sarcomeres. We conclude that El Bagre-EPF patients display autoreactivity to multiple cardiac

Correspondence to: Ana Maria Abreu-Velez, abreuvelez@yahoo.com.

Conflict of Interest None.

epitopes, that this disease may resemble what is found in patients with rheumatic carditis, and further, that the cardiac pathophysiology of this disorder warrants further evaluation.

Keywords

Heart; area composita; plakins; cell junctions; endemic pemphigus foliaceus; autoimmunity

Introduction

We have described a new variant of endemic pemphigus foliaceus in Colombia (El Bagre-EPF) with strong autoreactivity to numerous plakin molecules, including desmoplakins I and II (DP I–II), envoplakin, and periplakin [1–3]. Autoreactivity was also detected to desmoglein 1 (Dsg1) and desmoglein 3 (Dsg3), as well as to collagen type XVII [1–3]. We observed that selected El Bagre-EPF patients experienced a sudden death syndrome, occurring in about 14% of the patients younger than 50 years [1–3]. The sudden death events occurred with no prodromic symptoms, except for rapid syncope and generalized weakness for approximately 10 min.

Based on data that El Bagre-EPF patients share several autoantigens with patients affected with (1) paraneoplastic pemphigus (PNP) [4–6] and (2) paraneoplastic multiorgan syndrome [4–6] (including multiple plakin molecules present in cardiac tissue that are known to be antigens detected by El Bagre-EPF sera) [1–6], we tested for autoreactivity of El Bagre-EPF serum to the heart. We utilized cardiac tissue from multiple animal species, including rat, mouse, chipmunk, lamb, human, cow, pig, and chicken as antigen sources. We tested 15 El Bagre-EPF patient sera and 15 control sera from the endemic area, using direct and indirect immunofluorescence (DIF and IIF), immunohistochemistry (IHC), confocal microscopy (CFM), hematoxylin and eosin (H&E) histology, immunoblotting (IB), and immunoelectron microscopy (IEM).

Methods

Subjects of Study

We studied 15 patients who fulfilled the diagnosis of El Bagre-EPF. A clinical stage with histopathologic correlation was obtained, as described elsewhere [1– 3, 7]. The 15 cases fulfilled the following criteria: (a) patients displayed clinical features described for El Bagre-EPF [1–3, 7]; (b) patients lived in the endemic area; (c) patients' serum displayed ICS between keratinocytes and to the BMZ of the skin by either DIF or IIF, specifically using fluorescein isothiocyante (FITC)-conjugated monoclonal antibodies to human IgG4, or to total IgG in skin as described elsewhere [1–3]; (d) patient serum was positive by IB for reactivity against Dsg1, as well as for plakin molecules as previously described [1–3]; (e) patient serum immunoprecipitated a concanavalin A affinity-purified bovine tryptic 45 kDa fragment of the Dsg1 protein [8]; and (f) patient serum yielded a positive result using an enzyme-linked immunosorbent assay (ELISA) when screening for autoantibodies to pemphigus foliaceus (PF) antigens [9]. For all the above determinations, serum from a well-characterized EPF patient from Brazil and three patients with sporadic PF were used as positive controls. We also tested 15 controls from the endemic area matched by age, sex, and work activities. A human assurance review board approved the studies.

Skin Samples for Diagnosing El Bagre-EPF Disease

Following local anesthesia, skin biopsies were taken from affected areas. Written consents were obtained from all patients, and Institutional Review Board permission from the Hospital Nuestra Señora de El Carmen, in El Bagre, Colombia was obtained.

Heart Tissue from Three Patients with El Bagre-EPF

We obtained tissue from three patient necropsies and embedded part in optimal cutting temperature (OCT) compound and part in 10% formalin, following appropriate consent.

DIF and IIF

To identify the presence of autoantibodies in skin biopsies and heart tissues, we prefixed the samples with 3.5% paraformaldehyde, cut tissue at 4 μm thicknesses, washed, permeabilized with 0.1% Triton X-100, and blocked with 3% goat serum. Next, we incubated the tissues with the serum and/or the commercial antibodies used as markers. The tests were performed as previously described. For cell junction colocalizations, we used Connexin 43 for gap junctions (Sigma Aldrich, Saint Louis, MO, USA), DP I–II for the area composita (Serotec, Bavaria, Germany and Progen Biotechnik, Heidelberg, Germany), as well as Dsg1 and Dsg3 (Invitrogen). Pan-cadherin was utilized for desmosomes (Abcam, Inc., Cambridge, MA, USA). For tight junctions, we used junctional adhesion molecule A (JAM-A) and ezrin (Invitrogen). For blood vessels, we utilized ICAM-1/CD54 (Lab Vision Corporation, Fremont, CA, USA). For sarcomeric colocalization, we used anti-α-sarcomeric actin (Sigma Aldrich). Lastly, to study neural structures, we used the antibody to anti-glial fibrillary acidic protein (GFAP) conjugated with Cy3 (Sigma Aldrich). All sections were examined with a Nikon Eclipse 50i microscope (Japan). Some slides were counterstained with 4′,6-diamidino-2-phenylindole (DAPI) (Pierce, Rockford, IL, USA). Autofluorescence of lipofuschin A in the heart was taken into consideration in the analysis of the DIF, IIF, and CFM data.

Semiquantitative Image Analysis and Confocal Microscopy Imaging

To further study the possible reactivity and colocalization of patient autoantibodies with cardiac nerves, blood vessels, desmosomes, adherens and tight junctions, area composita, and sarcomeric fibers, we utilized confocal microscopy. Each photoframe included an area of approximately 440 × 330 μm. Fluorescent areas of each cell junction type were measured. A binary overlay was created automatically by a set threshold of 50 on a 255-point gray scale. We utilized a Nikon microscope with an EZC1 thumbnailer. All digital images were transferred to a tagged image file.

IHC

To colocalize patient autoantibodies, we also utilized IHC with a dual endogenous peroxidase blockage and an Envision dual link, according to Dako specifications. We tested for anti-human IgG, IgA, IgM, IgD, IgE, complement/C1q, complement/C3c, complement/C3d, albumin, fibrinogen, kappa, lambda, CD4, CD5, CD7, CD20, CD31, CD34, CD45, CD57, CD68, mast cell tryptase (MCT), alpha-1 anti-trypsin, HLA DP/DQ/DR, von Willenbrand factor, D2–40, matrix metalloproteinase 9, serotonin, class II MHC, myeloid/histiocyte antigen, HAM 56, calcitonin, p53, cyclin D1, myeloperoxidase, Ki-67 antigen, chromogranin A, vimentin, desmin, S-100 proteins, GFAP, neuron-specific enolase, myelin basic protein, anti-neurofilament, and protein gene product 9.5 (PPG 9.5) (all from Dako). Tests were performed as previously described [7, 10].

IEM

This was performed as previously described [10].

Mouse and Rat Heart Preparations for DIF, IIF, and CFM

Hearts were excised under ether anesthesia and fixed by perfusion of 2% paraformaldehyde with 0.01 mol/L PBS (via the coronary arteries) for 5 min. Hearts were then transversely sectioned and gradually infiltrated with Tissue- Tek OCT compound (Sakura Finetek, Japan). The specimens were then frozen and stored at −70°C until use.

IB

For IB, we utilized beef, mouse, and rat hearts. As controls, we used antibodies against DP I, DP II, Dsg1, and Dsg3, as previously described [1–6]. IB was performed utilizing an ECL set (SuperSignal West Pico chemioluminiscent substrate Western blotting kit) (Pierce) on 4% and 7% precasted gels (Invitrogen) [1–6]. Samples were separated by both 4% and 7% SDS-PAGE according to the Laemmli method [1–6]. Gels were transferred onto a nitrocellulose membrane.

Results

Our results showed a heterogeneous pattern of polyclonal autoreactivity that we subdivided based on the patterns and structures identified as positive. Human heart from the El Bagre-EPF necropsies showed the strongest reactivity by DIF and IIF; however, beef, mouse, rat, pork, veal, and chipmunk hearts were also positive, confirming that the cardiac immunoreactivity was directed against conserved molecules in multiple species. Chicken tissue was the least reactive. The most common observed pattern of reactivity was directed against the transverse tubule system (TTS). In addition, we found reactivity to gap, adherens, desmosomal, and tight junctions based on colocalization with the IIF, DIF, and CFM studies. We also found positivity to the area composita, blood vessels, and nerves, including the Purkinje system. We further detected a sarcomeric type of autoreactivity in one third of the El Bagre-EPF patients. The autoantibodies were polyclonal, as determined by CFM, DIF, IIF, and IHC (see Figs. 1, 2, 3, 4, and 5).

The human heart necropsy tissue from El Bagre-EPF patients revealed infiltration of some antigen-presenting cells, as determined by both H&E and IHC staining for S-100, myeloid/histoid, and HAM 56 markers (Figs. 1, 2, and 3). The IHC studies failed to confirm any B or T lymphocytic infiltration within the heart. Some paucicellularity of neural elements was also noted. Figure 1g shows fibrolipomatous replacement of about 15% of the right ventricular myocardium, which resembles some of the pathologic changes present in arrhythmogenic right ventricular cardiomyopathy (ARVC). The necropsy findings thus provide initial evidence that El Bagre-EPF autoantibodies contributed to the fibrolipomatous replacement. In addition, we confirmed El Bagre-EPF disease alterations by IHC within the autopsy cardiac tissue, utilizing the following markers: monoclonal mouse anti-human HLA DPDQDR antigen, polyclonal rabbit anti-human alpha-1 anti-trypsin, monoclonal mouse anti-human CD117/c-Kit, monoclonal mouse anti-human mast cell tryptase, polyclonal rabbit anti-human fibrinogen, polyclonal rabbit complement/C1q polyclonal rabbit anti complement, polyclonal rabbit anti-human albumin, polyclonal rabbit antihuman IgE, polyclonal rabbit anti-human IgM, and IgG.

We observed a compartmentalization of vinculin, as well as the strong presence of myeloperoxidase, MCT, and alpha-1 anti-trypsin, indicating active damage to the cardiac tissue. Masson’s trichrome, Verhoeff elastin, and H&E staining displayed a loss of collagen, elastin, and interstitial tissue. No necrosis or apoptosis was appreciated, although some p53 staining was observed. Figure 1 shows the most common patterns of autoreactivity detected in the sera of the El Bagre-EPF patients, including TTS involvement. We found that 7/15 of El Bagre patients displayed a polyclonal response to TTS, with the strongest reactivity

observed with anti-human fibrinogen (7/7), followed by anti-human IgG (6/7), anti-human complement/C3c (6/7), and anti-human albumin (5/7). In few cases, we found reactivity using antihuman IgM. We also found reactivity in 1/15 controls from the endemic area. The TTS reactivity was symmetrically distributed and was observed against all species investigated. Of interest, in the only control from the USA (a smoker with a history of two myocardial infarctions and a high serum cholesterol level), we detected strong deposits of autoantibodies to the TTS, specifically with FITC-conjugated anti-human fibrinogen and anti-human IgM antibodies.

The second most common pattern of reactivity was reactivity to blood vessels and the area composita of the heart, demonstrated by colocalization with ICAM-1/CD54 and DP I and II, respectively. In Fig. 1a, we used FITC-conjugated anti-human fibrinogen antibody to highlight intercellular reactivity (white dots, red arrow). The round structures (blue arrow) seem to be a series of TTS “virtual spaces”. Figure 1b shows positivity against the TTS in proximity to the area composita using FITC-conjugated anti-human IgG antibody. Figure 1c shows two types of reactivity using FITC-conjugated anti-human IgG antibodies: one is observed against round structures and the second directed against smaller cell junctions. Figure 1e shows a CFM image, demonstrating the reactivity to the TTS utilizing FITC-conjugated anti-human IgG antibody. Figure 1j shows an IEM picture of positive staining against heart mitochondria in a patient with El Bagre-EPF (blue arrows). The other reactivity (small black dots) is against the cell junctions. Figure 1k shows a diagram (with reproduction permission from reference [11]) displaying a model of the TTS. In Fig. 1g–i, some direct pathologic alterations found in the heart necropsies from El Bagre-EPF using H&E, Masson’s trichrome, and Verhoeff elastin are shown.

Figure 2 shows reactivity to the area composita of the heart, a common pattern observed in El Bagre-EPF patients. The reactivity was seen utilizing anti-human fibrinogen (7/7) followed by anti-human IgG (5/7), anti-human complement/ C3c (5/7), and anti-human albumin (5/7). In these cases, all the sera precisely colocalized with the antibody to DP I–II from Progen. Some reactivity overlapped between the area composita, the TTS, and other cell junctions. Figure 2a shows a CFM image demonstrating this overlap. The white arrows show the autoreactivity (green dots), utilizing FITC-conjugated anti-human IgG. In Fig. 2b, the confocal colocalization data of Fig. 2a indicate that the two antibodies to DP I–II from Progen (red staining) colocalize precisely with the patient antibodies (green staining). Panels d and g of Fig. 2 show tissue fracture electron microscopy images, displaying a series of cell junctions that are currently considered the area composita (white arrows) (reproduced with permission from the *Journal of Cell Science*, volume 10, pages 211 and 227, 1979; original Figures 9 and 10, from reference [12]). In Fig. 2h, an IEM ultraphotograph of the heart shows an El Bagre-EPF patient serum labeled with 10 nm gold-conjugated protein A present in several parts of the heart, i.e., the area composita, the desmosomes, the adherens junctions, and an area that resembles either gap or tight junctions. Figure 2i demonstrates positive El Bagre-EPF patient IHC stained with complement/C1q, indicating an immune response within the heart.

In Fig. 2, we detected reactivity to sarcomeric fibers, colocalizing the myosin antibody with anti-human IgG (5/7), anti-human complement/C3c (4/7), and anti-human IgM (2/7). In addition, we tested by IHC some pathological markers that could indicate direct damage and/or inflammation to the hearts from necropsies of El Bagre-EPF patients. Indeed, we detected positivity to MCT, alpha-1 anti-trypsin, myeloid/histoid cells, CD68, HAM 56, and to anti-human IgG, IgM, IgE, kappa, lambda, fibrinogen, and myeloperoxidase. Thus, our data support the concept of active antigen-presenting cells and a polyclonal immune response directed against heart tissue. In addition, we were able to see reactivity to several

heart nerve fibers (including Purkinje fibers), whose nature was confirmed by exact colocalization with antibodies to desmoplakins 1 and 2.

Figure 4 shows reactivity to gap and tight junctions, utilizing anti-human fibrinogen (5/7), anti-human IgG (6/7), anti-human complement/C3c (4/7), and anti-human albumin (1/7) antibodies. In Fig. 4a, a CFM image shows positive staining to the Purkinje fibers with one El Bagre-EPF serum. In Fig. 4e, we show positive reactivity to the lateral area of the myocytes where the mitochondria are located. In addition, we were able to demonstrate by IHC from El Bagre-EPF patient necropsy tissue positive staining to anti-human HLA DPDQDR and to anti-human HAM 56. In Fig. 4g, we show a representative immunoblot of heart tissue extract. In the heart IB, the blue arrows at the right show (in descending order) reactivity against 300, 250, 210, 190, 133, 120, and 97 kDa molecules in the sera from 7/15 El Bagre-EPF patients. The large blue arrow highlights a triplet of positive antigens, aggregated in the 210-kDa region. One control from the endemic area also showed positive staining to an antibody of 250 kDa. The positive bands observed in the El Bagre-EPF sera comigrated with the antibodies to the DP I–II controls at 250 and 210 kDa, respectively. Further, the 210- and 190-kDa bands comigrated with PNP sera bands corresponding to periplakin and envoplakin, respectively. Interestingly, we also noted that selected Progen commercial antibodies precisely matched the molecular weights of several of our El Bagre-EPF serum bands following immunoblotting. Specifically, precise matches were noted between our El Bagre-EPF serum bands and Progen antibody bands for velo-cardio-facial syndrome (ARVCF), desmoplakins I and II, and plakophilin 4 (p0071). A correlation p value of less than 0.05 was found vis-a-vis the matches of all of these bands. In addition, a 10% SDS-PAGE electrophoresis displayed bands of 90, 55, 45, and 34 kDa, specifically detected in El Bagre-EPF patients (data not shown). In Fig. 4h, a CFM image also displays positive staining to ICAM-1/CD54, colocalizing with the El Bagre-EPF autoantibodies.

Minor reactivity to the tight junctions of the heart (colocalizing with both ezrin and JAM-A) was also observed; reactivity was noted utilizing anti-human fibrinogen (4/7), anti-human IgG (3/7), and anti-human complement/C3c (4/7).

Figure 5 summarizes the multiple patterns of reactivity detected using El Bagre-EPF sera against heart tissue. We faced difficulty in elucidating these patterns because pattern overlap was observed. One example was desmosomal and/or gap junction signals overlapping with parts of the area composita. Figure 5a shows a sarcomeric pattern of reactivity and an autoreactivity to the area composita colocalizing with DP I–II. Figure 5b shows a cardiomyocyte from a necropsy of one El Bagre-EPF patient, combining Nomarski differential interference contrast confocal microscopy (NDIC) data, collected simultaneously with a classic CFM image. Most of the time, the El Bagre-EPF patient sera reactivity seemed to overlap with multiple cell junctions, especially with the area composita. In contrast, the antibodies to the sarcomere detected in the El Bagre-EPF serum seemed only to colocalize with myosin antibodies. Indeed, we were able to differentiate by immunoelectron microscopy the reactivity to the cell junctions versus reactivity to the muscle fibers (see Fig. 5f).

Discussion

The purpose of our study was to demonstrate the presence of autoantibodies to heart tissue in patients affected by El Bagre-EPF and their possible implications in the occurrence of sudden death in these patients. We detected multiple patterns of polyclonal reactivity to several parts of the heart; the most commonly observed pattern was directed against the TTS.

Other autoreactivity was found against the blood vessels and area composita of the heart. Of interest was the fact that the El Bagre-EPF reactivity was very similar to that obtained utilizing antibodies to DP I and DP II, ARVCF, desmoplakins I and II, and plakophilin 4 (p0071) from Progen. Other patterns of autoreactivity were found to gap junctions, adherens junctions, tight junctions, and overlapping areas of these structures. We further demonstrated colocalization of the patient antibodies with blood vessels, cardiac sarcomeres, and Purkinje fibers. We were able to demonstrate relevant pathological and immunological damage in cardiac tissue from necropsies of three El Bagre-EPF patients, indirectly indicative that heart tissue is being altered by the immune response to this organ. As previously demonstrated in patients with paraneoplastic pemphigus, we found strong reactivity to cardiac tissue, possibly due to the high content of plakins within this organ [1–6]. Skin and heart tissues are subject to shear mechanical stress, thus necessitating both stress resistance and mechanical flexibility [5]. Many intercellular connecting structures in the skin and heart such as the gap and adherens junctions, desmosomes, and recently described area composita resist these forces and display remarkable ultrastructural conservation in multiple species vis-a-vis the skin and heart [13]. The area composita represents a special, muscle-specific type of adherens junction, connecting cardiac myocytes; it assists in force transmission during contraction of the mammalian cardiac intercalated disks [14, 15].

Mutations in desmosomal proteins may lead to inherited cardiocutaneous syndromes such as Naxos disease/MIM601214, and Carvajal syndrome/MIM605676 (caused by complete deficiencies and/or mutations in plakoglobin, desmoplakin, or desmogleins) [16–19]. Thus, the skin and palmoplantar syndromes associated with cardiac alterations could be etiologically related [16, 19]. Notably, patients affected by Brazilian endemic pemphigus foliaceus, as well as by El Bagre-EPF, often present clinically with some degree of palmoplantar keratoderma and often exhibit genetic consanguinity and clustering [10, 20, 21].

In addition, other studies have indicated that cell junctions and their constituent molecules play a role in inherited cardiomyopathies such as ARVC [22, 23]. One study suggested that ARVC represents a disease of the intercalated disks and desmosomes of the heart [22, 23]. In our future research, we aim to compare pathologic and immunologic profiles in patients affected by El Bagre-EPF, ARVC, and other cardiocutaneous syndromes.

We suggest that the sudden death syndrome seen in some of the El Bagre-EPF patients may be due to the presence of autoantibodies against the cardiac Purkinje system and desmosomes and, further, possibly manifested due to their indirect role in maintaining physiologic conductivity via modulation of gap junctions [24].

It has been shown that bullous pemphigoid antigen 1 (BPAG1) (also one of the El Bagre-EPF antigens) is a member of the plakin family, with cytoskeletal linkage properties [25–27]. Mutations in BPAG1 may cause sensory neuron degeneration and skin fragility in mice [25–27]. Alternative splicing within the BPAG1 locus produces multiple protein isoforms from specific cytoskeletal linkage domains, altering the predominant isoforms in neurons and muscles [25–27]. Based on this information and our findings, we suggest that autoantibodies in El Bagre-EPF patients may affect the conductance system in the heart. We recently described autoantibodies to the nerves and mechanoreceptors in patients affected by this disorder (Abreu Velez et al., manuscript submitted). The presence of autoantibodies to Purkinje cells in this study may also help explain the sudden death syndrome, as shown in patients with damage to these fibers experiencing atrioventricular heart block, and or arrhythmias [28, 29]. It is known that Ca^{++} enters the myocyte via Na^{+}–Ca^{++} transport exchange, with the interior of the myocyte becoming positively charged and resulting in

Ca^{++} influx and Na^{+} efflux. Studies have suggested that this transporter is located in the TTS and in the sarcolemma. Several El Bagre-EPF antigens are calcium dependent, including desmogleins 1 and 3 [8]. The TTS allow rapid propagation of excitation into the cell interior and is complex and reticular in nature [30–33]. Of interest, this system has received minimal attention recently, with many studies of the system found in older literature. Nevertheless, one recent study has shown that the voltage-gated K^{+} channel Kv4.2 localizes predominantly to the TTS of rat myocytes and may interface with other channels [34]. Of note, the conduction system of the heart is also calcium dependent [13]. In our study, we were able to demonstrate colocalization of patient El Bagre-EPF autoantibodies with several cell junctions of the heart, as well as against blood vessels, nerves, and the TTS. As a clinical correlation, we were able to study one electrocardiogram (EKG) from one El Bagre-EPF patient who displayed positive autoantibodies to the heart; the EKG evaluation was within normal limits. Further EKG and electrophysiological studies are warranted, given our results.

Also of note, cases of pemphigus vulgaris have been reported with extensive thrombosis of deep veins, pulmonary veins, and cardiac chambers, complicated by myocardial infarction [35, 36]. Preceding the therapeutic steroid era, the Brazilian literature reported alterations in the hearts at autopsy from patients affected by fogo selvagem [20]. In our current study, we document significant disease autoantigenicity in autopsy tissue from three El Bagre-EPF patients. We cannot rule out the possibility that the sudden deaths of these patients may have resulted from vascular thrombosis. Other explanations of the sudden deaths might include neural conductance problems such as atrioventricular heart block and/or arrhythmias or abnormalities present within their cardiac cell junctions [28, 29].

In regard to our positive antibodies to heart mitochondria, a review of 23 cases of pemphigus vulgaris noted some alterations in the mitochondria, the site of NADH2–cytochrome c reductase activity [37]. In addition, apoptolysis in pemphigus vulgaris seems to be a complex process initiated by at least three classes of autoantibodies directed against desmosomal, mitochondrial, and other keratinocyte self-antigens [38].

Another theory to explain the presence of heart autoantibodies in El Bagre-EPF arises from the example of group A *Streptococcus* infection, where the host immunologic response to bacterial antigens cross-reacts with various target organs (including the heart), due to molecular mimicry [12]. In fact, autoantibodies reactive against the heart have been found in patients with rheumatic carditis [12]. Currently, this mechanism cannot be ruled out in the pathophysiology of El Bagre-EPF; an unknown environmental antigen could play a similar antigenic role.

Previous studies have shown a significant role for autoantibodies in selected cardiac diseases [11, 39, 40]. Further, anti-cardiac autoantibodies have been identified not only in the sera of patients with heart diseases, but also in low titers in some healthy individuals [11, 39, 40]. Further, the complete role of these antibodies in the development of autoimmune heart disease has not been fully elucidated. Highlighting one example, anti-myosin autoantibodies are present in multiple heart diseases, including myocarditis, dilated cardiomyopathy, Chagas' disease, Kawasaki disease, rheumatic fever, and ischemic myocardium. The pathogenic role(s) of anti-myosin autoantibodies in these diverse cardiac diseases is currently not well defined. Similarly, the clinical implications of the cardiac autoantibodies in El Bagre-EPF disease remain to be determined. Antibody cross-reactivity could play a role in the pathophysiology of these diseases; myosin autoantibodies have been previously documented as cross-reacting with the β-adrenergic receptor [11, 39, 40].

Indeed, a large necropsy study with 56 patients affected by pemphigus before the steroid era supports our data. The authors described several lesions in the hearts of these patients, including multiple cardiovascular alterations seen at different anatomic levels of the heart. The most common were pericarditis, lipid degeneration of the vessels, parenchymatosis of the heart walls, chronic endocarditis of the valves including verrucous endocardioathasis, dark atrophy of the cordis (atrophia brunea cordis), chronic myocarditis, and atherosclerosis of some vessels [41]. Proposed future studies include correlations of (1) El Bagre-EPF disease EKG data and (2) presence of anti-cardiac antibodies with both the likelihood of sudden death in these patients and with pertinent cardiac enzyme fluctuations.

In conclusion, we note that (1) both skin as well as muscle (skeletal, smooth, and cardiac) have desmosomes and complex cell junctions; (2) skin and muscle have different isoforms of plakins and desmogleins; (3) several syndromes display impairment of these molecules in both skin and heart, and the genes affected in these disorders encode proteins such us plakoglobin, plakophilin, desmogleins, desmocollin, and desmoplakin, which are also pemphigus and paraneoplastic pemphigus antigens; (4) patients affected by multiorgan paraneoplastic syndromes share similar autoantibodies with El Bagre-EPF patients (such as those to plakins); (5) both the skin and heart are subject to significant shear mechanical stress and thus need to provide flexible mechanical resistance; and (6) both skin and heart are rich in several specialized neural structures that are essential to survival of the species. We suggest that multiple cell junctions are targets of El Bagre-EPF antibodies. Further studies will be needed to address the specific pathogenic effects of these antibodies in both in vitro and in vivo models and the reasons for their diverse polyclonality. In addition, further testing is needed to identify specific neural pathologic sequelae of this disorder, including possible damage to Purkinje cells and other neural elements of the cardiac conduction system.

Acknowledgments

Funding Sources This study was supported by Georgia Dermatopathology Associates, Atlanta, Georgia, USA (MSH). The El Bagre-EPF samples were collected through previous grants from the University of Antioquia, the Embassy of Japan in Colombia, the Mineros de Antioquia SA, DSSA, the Hospital Nuestra Senora del Carmen, all in Medellin, Colombia, South America (AMAV). H & E, IHC, DIF, IIF, and IEM studies were funded by Georgia Dermatopathology Associates (MSH and AMAV). Confocal studies were performed with funds from the Department of Ophthalmology, Emory University Medical Center, Atlanta, Georgia, USA (HG) (NIH NEI EY06360) and P01 HL058000 from (SCD).

Abbreviations

BMZ	Basement membrane zone
EPF	Endemic pemphigus foliaceus
El Bagre-EPF	El Bagre endemic pemphigus foliaceus
ICS	Intercellular staining between keratinocytes
IB	Immunoblotting
DIF	Direct immunofluorescence
IIF	Indirect immunofluorescence
TTS	Transverse tubule system
IEM	Immunoelectron microscopy
H&E	Hematoxylin and eosin

ARVC	Arrhythmogenic right ventricular cardiomyopathy

References

1. Abréu-Vélez AM, Beutner EH, Montoya F, Bollag WB, Hashimoto T. Analyses of autoantigens in a new form of endemic pemphigus foliaceus in Colombia. J Am Acad Dermatol. 2003; 49:609–614. [PubMed: 14512904]
2. Abréu-Vélez AM, Hashimoto T, Bollag WB, et al. A unique form of endemic pemphigus in Northern Colombia. J Am Acad Dermatol. 2003; 4:599–608.
3. Hisamatsu Y, Abreu Velez AM, Amagai M, Ogawa MM, Kanzaki T, Hashimoto T. Comparative study of autoantigen profile between Colombian and Brazilian types of endemic pemphigus foliaceus by various biochemical and molecular biological techniques. J Dermatol Sci. 2003; 32:33–41. [PubMed: 12788527]
4. Sehgal VN, Srivastava G. Paraneoplastic pemphigus/paraneoplastic autoimmune multiorgan syndrome. Int J Dermatol. 2009; 48:162–169. [PubMed: 19200194]
5. Mahoney MG, Aho S, Uitto J, Stanley JR. The members of the plakin family of proteins recognized by paraneoplastic pemphigus antibodies include periplakin. J Invest Dermatol. 1998; 111:308–313. [PubMed: 9699735]
6. Anhalt GJ, Kim SC, Stanley JR, et al. Paraneoplastic pemphigus. An autoimmune mucocutaneous disease associated with neoplasia. N Engl J Med. 1990; 323:1729–1735. [PubMed: 2247105]
7. Howard MS, Yepes MM, Maldonado-Estrada JG, et al. Broad histopathologic patterns of non-glabrous skin and glabrous skin from patients with a new variant of endemic pemphigus foliaceus—part 1. J Cutan Pathol. 2010; 37:222–230. [PubMed: 19615020]
8. Abreu-Velez A, Javier Patino P, Montoya F, Bollag W. The tryptic cleavage product of the mature form of the bovine desmoglein 1 ectodomain is one of the antigen moieties immunoprecipitated by all sera from symptomatic patients affected by a new variant of endemic pemphigus. Eur J Dermatol. 2003; 4:359–366. [PubMed: 12948916]
9. Abréu-Vélez AM, Yepes MM, Patiño PJ, Bollag WB, Montoya F Sr. A cost-effective, sensitive and specific enzyme linked immunosorbent assay useful for detecting a heterogeneous antibody population in sera from people suffering a new variant of endemic pemphigus. Arch Dermatol Res. 2004; 295:434–441. [PubMed: 14730452]
10. Abreu Velez AM, Howard MS, Hashimoto T. Palm tissue displaying a polyclonal autoimmune response in patients affected by a new variant of endemic pemphigus foliaceus in Colombia, South America. Eur J Dermatol. 2010; 20:74–81. [PubMed: 19889592]
11. Nussinovitch U, Shoenfeld Y. The diagnostic and clinical significance of anti-muscarinic receptor autoantibodies. Clin Rev Allergy Immunol. 2011 (in press).
12. Malnick SD, Bar-Ilan A, Goland S, Somin M, Doniger T, Basevitz A, et al. Perimyocarditis following streptococcal group A infection: from clinical cases to bioinformatics analysis. Eur J Intern Med. 2010; 21:354–356. [PubMed: 20603051]
13. Bolling MC, Jonkman MF. Skin and heart: une liaison dangereuse. Exp Dermatol. 2009; 18:658–668. [PubMed: 19558499]
14. Borrmann CM, Grund C, Kuhn C, Hofmann I, Pieperhoff S, Franke WW. The area composita of adhering junctions connecting heart muscle cells of vertebrates. II. Colocalizations of desmosomal and fascia adhaerens molecules in the intercalated disk. Eur J Cell Biol. 2006; 85:469–485. [PubMed: 16600422]
15. Pieperhoff S, Franke WW. The area composita of adhering junctions connecting heart muscle cells of vertebrates—IV: coalescence and amalgamation of desmosomal and adhaerens junction components—late processes in mammalian heart development. Eur J Cell Biol. 2007; 86:377–391. [PubMed: 17532539]
16. Milingou M, Wood P, Masouyé I, et al. The palmoplantar keratodermas: much more than palms and soles. Mol Med Today. 1999; 5:107–113. [PubMed: 10203734]

17. Barber AG, Wajid M, Columbo M, Lubetkin J, Christiano AM. Striate palmoplantar keratoderma resulting from a frameshift mutation in the desmoglein 1 gene. J Dermatol Sci. 2007; 45:161–166. [PubMed: 17194569]
18. Kelsell DP, Stevens HP. The palmoplantar keratodermas: much more than palms and soles. Mol Med Today. 1999; 5:107–113. [PubMed: 10203734]
19. Wan H, Dopping-Hepenstal PJ, Gratian MJ, et al. Striate palmoplantar keratoderma arising from desmoplakin and desmoglein 1 mutations is associated with contrasting perturbations of desmosomes and the keratin filament network. Br J Dermatol. 2004; 150:878–891. [PubMed: 15149499]
20. Abreu-Velez AM, Howard MS, Yi H, Gao W, Hashimoto T, Grossniklaus HE. Neural system antigens are recognized by autoantibodies from patients affected by a new variant of endemic pemphigus foliaceus in Colombia. J Clin Immunol. 2011; 31(3):356–368. [PubMed: 21210298]
21. Abreu-Velez AM, Villa-Robles E, Howard MS. A new variant of endemic pemphigus foliaceus in El-Bagre, Colombia: the Hardy–Weinberg–Castle law and linked short tandem repeats. North Am J Med Sci. 2009; 1:169–179.
22. Perriard JC, Hirschy A, Ehler E. Dilated cardiomyopathy: a disease of the intercalated disc? Trends Cardiovasc Med. 2003; 13:30–38. [PubMed: 12554098]
23. Awad MM, Calkins H, Judge DP. Mechanisms of disease: molecular genetics of arrhythmogenic right ventricular dysplasia/cardiomyopathy. Nat Clin Pract Cardiovasc Med. 2008; 5:258–267. [PubMed: 18382419]
24. Oxford EM, Musa H, Maass K, Coombs W, Taffet SM, Delmar M. Connexin 43 remodeling caused by inhibition of plakophilin-2 expression in cardiac cells. Circ Res. 2007; 101:703–711. [PubMed: 17673670]
25. Leung CL, Zheng M, Prater SM, Liem RK. The BPAG1 locus: alternative splicing produces multiple isoforms with distinct cytoskeletal linker domains, including predominant isoforms in neurons and muscles. J Cell Biol. 2001; 154:691–697. [PubMed: 11514586]
26. Leung CL, Sun D, Zheng M, Knowles DR, Liem RK. Microtubule actin cross-linking factor (MACF): a hybrid of dystonin and dystrophin that can interact with the actin and microtubule cytoskeletons. J Cell Biol. 1999; 147:1275–1286. [PubMed: 10601340]
27. Leung CL, Sun D, Zheng M, Knowles DR, Liem RK. The intermediate filament protein peripherin is the specific interaction partner of mouse BPAG1-n (dystonin) in neurons. J Cell Biol. 1999; 144:435–436. [PubMed: 9971739]
28. Ideker RE, Kong W, Pogwizd S. Purkinje fibers and arrhythmias. Pacing Clin Electrophysiol. 2009; 32:283–285. [PubMed: 19272054]
29. Obbiassi M, Brucato A, Meroni PL, et al. Antibodies to cardiac Purkinje cells: further characterization in autoimmune diseases and atrioventricular heart block. Clin Immunol Immunopathol. 1987; 42:141–150. [PubMed: 3802583]
30. Forssmann GF, Girardier L. A study of the T system in rat heart. J Cell Biol. 1970; 44:1–19. [PubMed: 4901374]
31. Lorber V, Rayns DG. Cellular junctions in the tunicate heart. J Cell Sci. 1972; 10:211–227. [PubMed: 5017426]
32. Soeller C, Cannell MB. Examination of the transverse tubular system in living cardiac rat myocytes by 2-photon microscopy and digital image-processing techniques. Cir Res. 1999; 84:266–275.
33. Nelson DA, Benson ES. On the structural continuities of the transverse tubular system of rabbit and human myocardial cells. J Cell Biol. 1963; 16:297–313. [PubMed: 13938025]
34. Takeuchi S, Takagishi Y, Yasui K, Murata Y, Toyama J, Kodama I. Voltage-gated K^+ channel, Kv4.2, localizes predominantly to the transverse–axial tubular system of the rat myocyte. J Mol Cell Cardiol. 2000; 32:1361–1369. [PubMed: 10860776]
35. Arnaout MS, Dimasi A, Harb R, Alam S. Unusual thrombotic cardiac complications of pemphigus vulgaris: a new link? J Thromb Thrombolysis. 2007; 23:237–240. [PubMed: 17186391]
36. Chorzelski T, Kuch J. Anticardiac antibodies and “pemphigus” autoantibodies in a patient with pemphigus and myocardial infarction. Pol Arch Med Wewn. 1968; 41:825–830. [PubMed: 4884430]

37. Gheorghe E, Adumitresi C, Botnarciuc M, Manea M. Histochemical study of the skin affected by certain autoimmune diseases. Rom J Morphol Embryol. 2005; 46:73–78. [PubMed: 16286989]

38. Marchenko S, Chernyavsky AI, Arredondo J, Gindi V, Grando SA. Antimitochondrial autoantibodies in pemphigus vulgaris: a missing link in disease pathophysiology. J Biol Chem. 2010; 285:3695–3704. [PubMed: 20007702]

39. Nussinovitch U, Shoenfeld Y. Anti-tropopin autoantibodies and the cardiovascular system. Heart. 2010; 96:1518–1524. [PubMed: 20837669]

40. Nussinovitch U, Shoenfeld Y. The clinical significance of antibeta-1 adrenergic receptor autoantibodies in cardiac disease. Clin Rev Allerg Immunol. 2011 (in press).

41. Földvári F, Baló J, Márton C. Anatomical-pathologic report of autopsies of 62 cases of pemphigus. Przegl Dermatol. 1967; 54:13–16. [PubMed: 5298817]

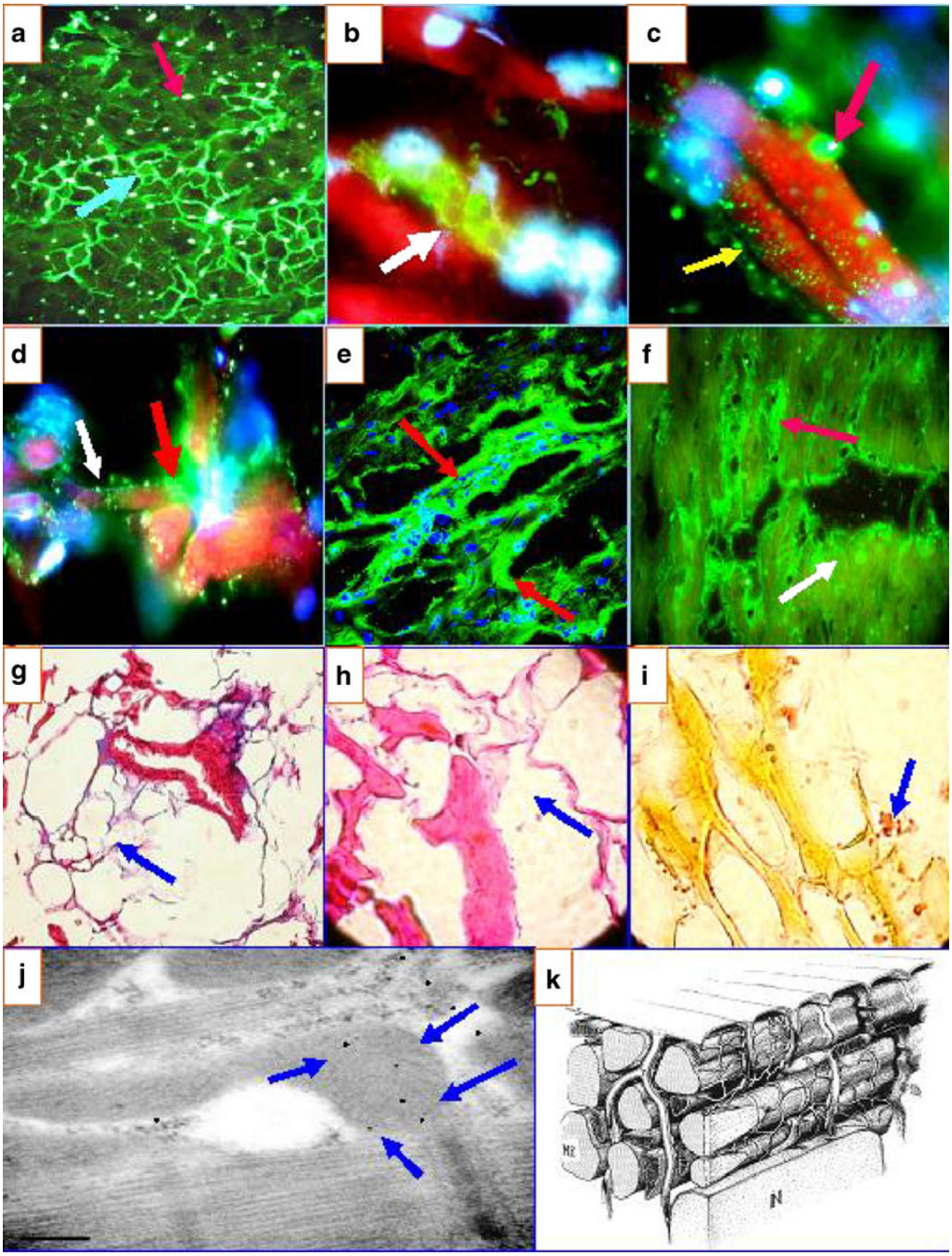

Fig. 1.

a Anti-human fibrinogen antibody conjugated with FITC highlight the intercellular reactivity to the area composita of the heart (*blue light arrow*). **b** Positivity against rounded structures in proximity to the TTS using FITC-conjugated anti-human IgG antibody (*green* reactivity) (*red arrow*). **c** Two types of reactivity using FITC-conjugated anti-human IgG antibodies: one is observed against the larger round structures (reactivity in *green*; *red arrow*) and another directed against smaller structures (*yellow arrow*). **d** The same antibody as in **c**, showing reactivity to the TTS (green staining) (*red arrow*) and to the smaller structures (*white arrow*). **e** a CFM image demonstrating the reactivity to the TTS (green

staining; *red arrows*) using FITC-conjugated anti-human IgG antibody. **f** Similar to **e** but at lower magnification. The *red arrow* shows the reactivity to the TTS, and the *white arrow* shows the reactivity to the smaller, round structures (faint yellow staining). In addition, in **g** (Masson's trichrome), **h** (H&E), and **i** (Verhoeff elastin), we show some representative pictures of the loss of collagen and elastin fibers and some replacement with lipomatous tissue, respectively (*blue arrows*). **j** IEM highlighting positive staining against the heart mitochondria in a patient with El Bagre-EPF (*blue arrows*). The other reactivity (*small black dots*) is against cell junctions. **k** A model of myocardial fibers, the components of the sarcoplasmic reticulum and their relationship with the TTS

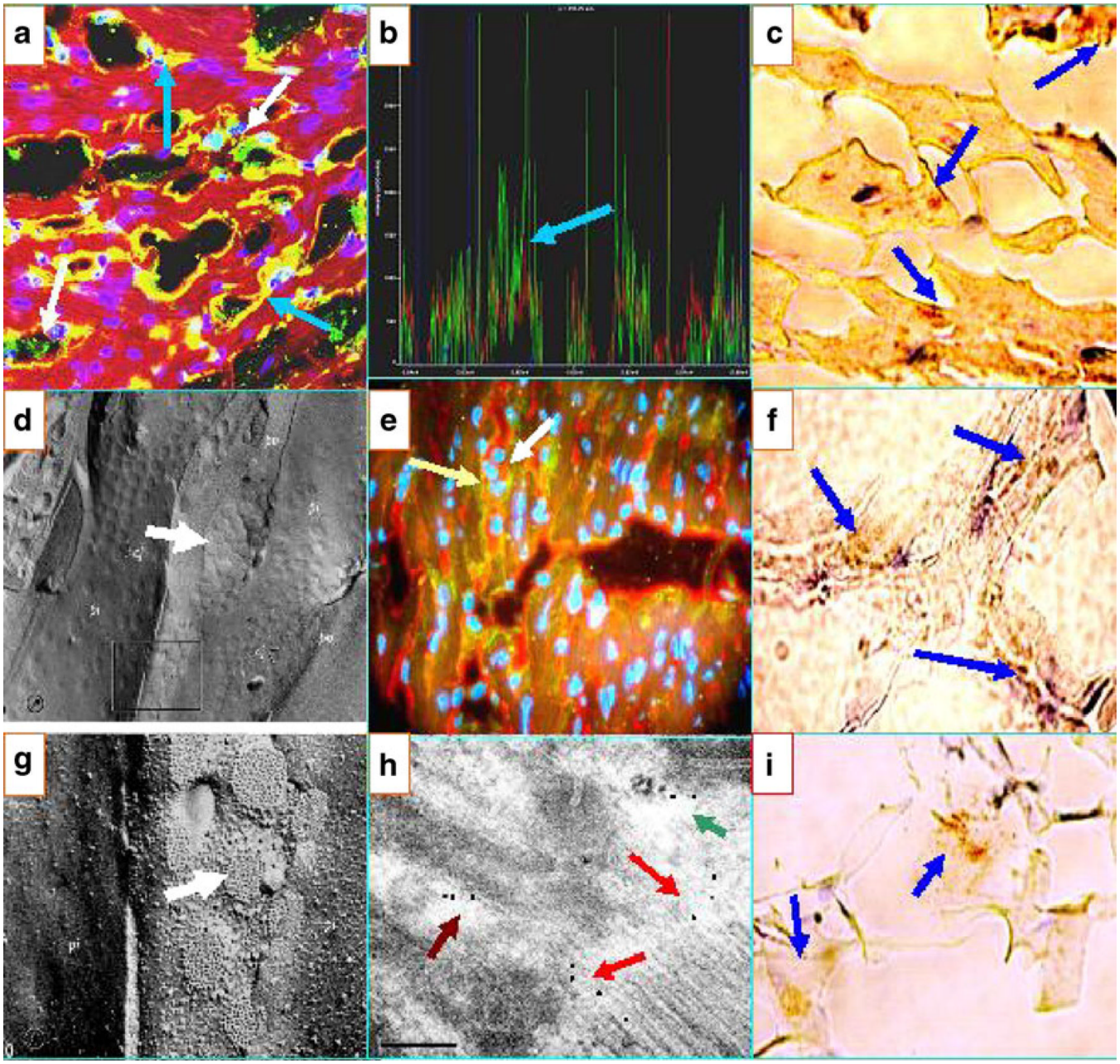

Fig. 2.

a Confocal image showing positivity against the area composita of the heart. The *white arrows* show *green dots* representing FITC-conjugated anti-human IgG antibody autoreactivity. The *blue arrows* show autoreactivity (yellow staining) to the TTS. The nuclei are counterstained in *purple* with DAPI. **b** CFM colocalization of the **a** peaks of fluorescence, indicating that the antibodies to DP I–II (red staining) colocalize with the patient antibodies (green staining; *blue arrow*). The *faint blue peaks* represent the DAPI nuclear counterstaining. **c** IHC showing positive staining of one El Bagre-EPF patient necropsy heart with anti-human IgE antibody (*blue arrows*; dark staining). **e** DIF showing colocalization of antibodies to Connexin 43 in *red* (*white arrow*) with an El Bagre-EPF patient serum (green staining; *light yellow arrow*). **d**, **g** Pictures from tissue fracture electron microscopy of the area composita (*white arrows*). **f** IHC showing positive staining within the

heart using anti-human fibrinogen antibody (*blue arrows*). **h** An IEM photograph of the heart showing El Bagre-EPF serum labeled with 10 nm gold-conjugated protein A antibodies, reacting with multiple heart structures including the area composita (*maroon arrow*; *black dots*), an interface area of the desmosomes and adherens junctions (*red arrows*), and an area that resembles either gap and/or tight junctions (*green arrow*) (100KX). **i** An IHC stain of El Bagre-EPF patient heart, staining positive with complement/C1q

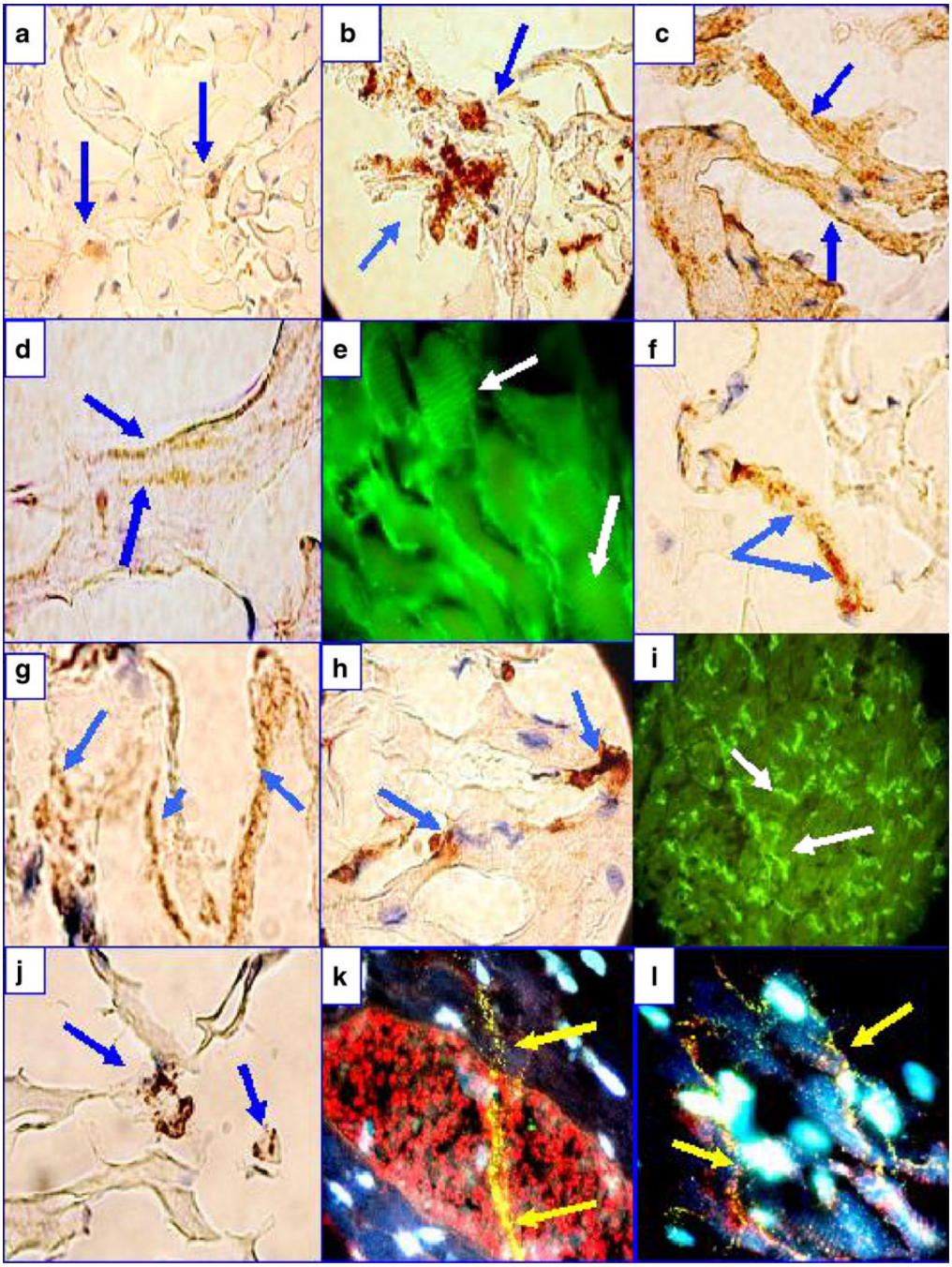

Fig. 3.

IHC and IIF of a heart from one El Bagre-EPF patient necropsy. **a** Anti-human IgG-positive IHC staining to the area composita of the heart (*blue arrows*; brown staining). **b** Positive IHC staining using anti-human HAM 56 antibody (brown staining; *blue arrows*). **c** Positive IHC staining against several areas of the heart using anti-human complement/C1q (*blue arrows*). **d** Positive IHC staining of the sarcomere using anti-human IgG (*blue arrows*). **e** IIF showing similar sarcomeric staining using anti-human IgG (*white arrows*). **f** Positive IHC staining of the heart using anti-human IgM (*blue arrows*). **g** Anti-human kappa light chains stained strongly positive (*blue arrows*). **h** Positive IHC staining for myeloperoxidase (brown

staining; *blue arrows*). **i** DIF showing positive staining along intermyocyte junctions (*white arrows*). **j** Positive IHC staining for mast cell tryptase (brown staining; *blue arrows*). **k** IIF showing the area composita, highlighted in *red* using Texas red-conjugated anti-DP I–II and positivity to a long linear structure (yellow staining; *yellow arrows*), utilizing FITC-conjugated anti-human IgM antibody. The linear structure was also faintly positive with DP I and DP II antibodies, precisely colocalizing with El Bagre-EPF autoantibodies against the Purkinje fibers. The nuclei are counterstained in *light blue* with DAPI. **l** Same as **k** but at lower magnification

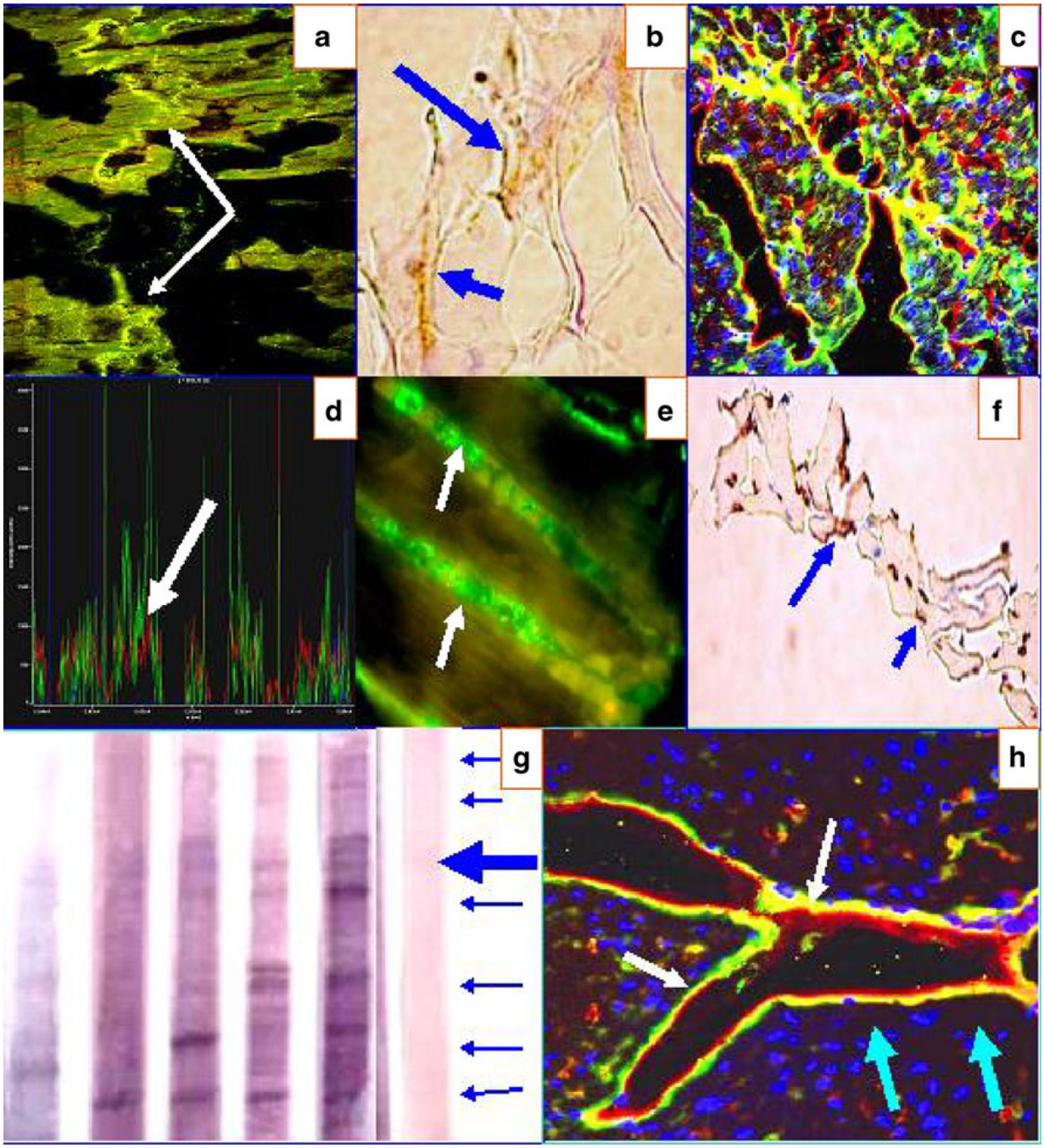

Fig. 4.

a CFM image showing positive staining to the Purkinje fibers (yellow bead-like dot staining) from one El Bagre-EPF patient serum (*white arrows*). **b** IHC from El Bagre-EPF patient necropsy heart staining positive to anti-human HLA DPDQDR antibody (brown staining; *blue arrows*). **c** Same as **a** at lower magnification. **d** CFM colocalization of the fluorescent peaks of the **a/c** data, showing that antibodies to Connexin 43 (red staining) colocalize precisely with the patient antibodies (green staining; *white arrow*). The *blue peaks* represent DAPI nuclear counterstaining. In **e**, we found positive reactivity to the lateral area of the myocytes (where mitochondria are located) using one El Bagre-EPF patient serum

(*white arrows*). **f** IHC from El Bagre-EPF patient necropsy heart, displaying positive staining to anti-human HAM 56 (brown staining; *blue arrows*). **g** An IB of heart tissue extract. The *blue arrows* at the *right* show (in descending order) reactivity against 300, 250, 210, 190, 133, 120, and 97 kDa molecules in the sera from El Bagre-EPF patients. The *large blue arrow* highlights a triplet of positive antigens, aggregated in the 210-kDa area. One control from the endemic area also showed positive staining to an antibody of 250 kDa. **h** CFM image showing positive staining in heart tissue to ICAM-1/CD54 (red staining; *light blue arrows*). The yellow/green staining represents reactivity of the patient autoantibodies using FITC-conjugated anti-human IgG antibodies (*white arrows*). Nuclei are again counterstained with DAPI (dark blue staining)

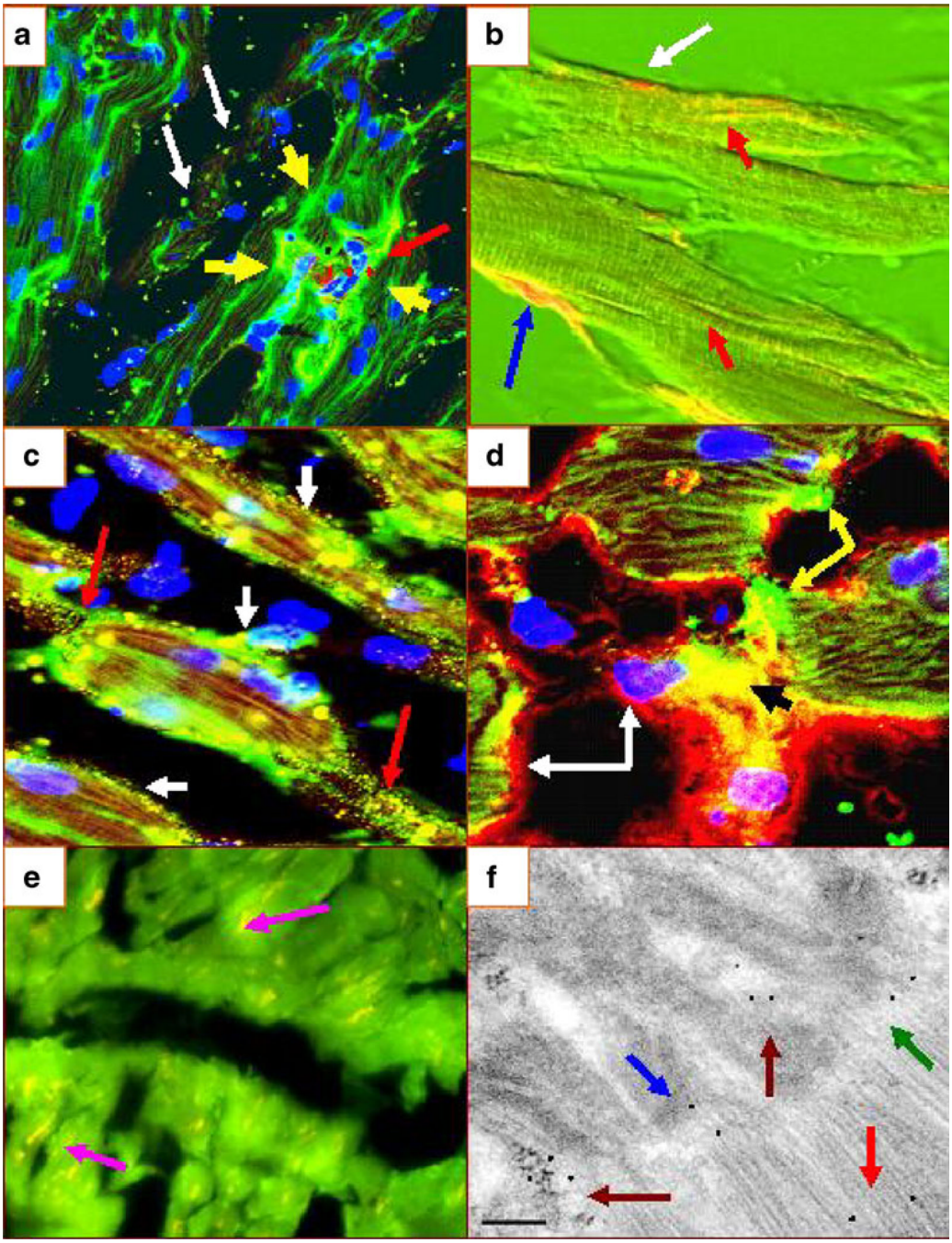

Fig. 5.

a DIF autoreactivity to the area composita (*green* reactivity using FITC-conjugated anti-human IgG antibody from one El Bagre-EPF patient) (*yellow arrows*), colocalizing precisely with DP I–II polyclonal antibodies (red staining; *red arrow*). The *white arrows* demonstrate dot staining to homogeneous large dense bodies (green staining). **b** Cardiac myocytes from a necropsy of one El Bagre-EPF patient, evaluated using NDIC. The *blue arrow* shows positivity to part of the TTS (yellow staining). The *red arrows* show reactivity to sarcomeric fibers (yellow staining), and the *white arrow* shows positivity to a gap junction (orange staining). **c** CFM image displaying positive yellow dot staining between the myocytes to

their intercalated disks (*red arrows*) and to several areas in the sarcolemma of the cardiac myocytes (yellow staining; *white arrows*). **d** Positivity using FITC-conjugated anti-human fibrinogen antibody to the area composita (green staining; *yellow arrows*) and to the TST area (yellow staining; *black arrow*). Please note the colocalization of ICAM/CD54 (red staining, *white arrows*). **e** A negative control stain (the *fuchsia arrows* show the yellowish, physiological staining of lipofuscin). Finally, in **f**, an IEM ultraphotograph of heart tissue showing El Bagre-EPF patient serum autoreactivity (using 10 nm gold-conjugated protein A labeling) to several structures of the heart, including the area composita (*maroon arrows*) (*black dots*), the sarcoplasmic muscle (*red arrow*), junctions between the desmosomes and the adherens junctions (*green arrow*), and to an area that resembles either gap and/or tight junctions (*blue arrow*) (100 kV)